P-glycoprotein protein expression versus functionality at the blood-brain barrier using immunohistochemistry, microdialysis and mathematical modeling

Lange, E.C.M. de; Berg, D.J. van den; Bellanti, F.; Voskuyl, R.A.; Syvänen, S.

European Journal of Pharmaceutical Sciences 124 (2018) 61–70

Contents lists available at ScienceDirect

European Journal of Pharmaceutical Sciences

journal homepage: www.elsevier.com/locate/ejps

P-glycoprotein protein expression versus functionality at the blood-brain barrier using immunohistochemistry, microdialysis and mathematical modeling

E.C.M. De Lange[a,*], D.J. vd Berg[a], F. Bellanti[b], R.A. Voskuyl[a,c], S. Syvänen[a,d]

[a] Division of Pharmacology, Leiden Academic Centre of Drug Research, Leiden University, the Netherlands
[b] Certara Strategic Consulting, Oss, the Netherlands
[c] Stichting Epilepsie Instellingen Nederland (SEIN), Heemstede, the Netherlands
[d] Department of Public Health and Caring Sciences/Geriatrics, Uppsala University, Uppsala, Sweden

ARTICLE INFO

Keywords:
P-glycoprotein
Protein expression
Functionality
Blood-brain barrier
Microdialysis
Kainate
Quinidine

ABSTRACT

A proper understanding of P-gp mediated transport (functionality) at the blood-brain barrier (BBB) and beyond is needed to interpret, understand and predict pharmacokinetic (PK)- pharmacodynamic (PD) relationships of CNS drugs that are substrates of P-gp, especially since P-gp functionality may be different in different conditions. Often, P-gp expression is taken as a biomarker of transporter functionality. The aim of our study was to investigate whether brain capillary protein expression of P-gp is associated with changes in P-gp mediated drug efflux at the BBB.

Status Epilepticus (SE) was induced by kainate in male rats. During 3–5 weeks post SE, hippocampal P-gp expression was determined using immunohistochemistry, while BBB P-gp functionality was assessed by microdialysis of quinidine, in absence and presence of the P-gp blocker tariquidar. The data were analyzed using Nonlinear Mixed Effect Modeling implemented in NONMEM.

Following SE, changes in brain capillary P-gp expression were observed. However, no relation between BBB P-gp protein expression and BBB P-gp mediated drug efflux was found. This warrants a critical view on the interpretation of reported changes in BBB P-gp expression as a biomarker of BBB P-gp functionality.

1. Introduction

Adequate drug distribution to the target site is a prerequisite for drug-target interaction and thereby drug effects. Apart from passive diffusion, active drug transport can have an important impact on drug distribution over different body compartments. Active transport depends on transporter functionality, which is condition dependent. (Erdö et al., 2017; Kervezee et al., 2014). This indicates that a proper understanding of transporter functionality is needed to interpret, understand and predict pharmacokinetic (PK)- pharmacodynamics (PD) relationships in different conditions. (de Lange et al., 2017).

Drug distribution into the brain is determined by both drug - and blood-brain barrier (BBB) properties (Yamamoto et al., 2018). The BBB contains many active transporters, and for any drug being a substrate of one of these transporters, the rate as well as extent of drug distribution into the brain can be influenced by active transport processes. P-glycoprotein is considered the most important efflux transporter at the BBB, having many drugs as substrates. Many studies have been devoted to understanding the impact of P-gp mediated BBB efflux in brain distribution of its substrates. Moreover, P-gp may be present not only at the BBB but also at brain parenchymal cells (Lee et al., 2001).

An in vivo technique that can be used to determine rate and extent of drug brain distribution is Positron Emission Tomography (PET). PET measures the total activity of a tracer, incorporated in the drug right before injection into the living subject. This technique has many advantages, such as being non-invasive (therefore can be used in humans) and providing time as well as spatial resolution, however, one of its disadvantages is that it cannot distinguish between bound and unbound drugs. This makes that BBB transport parameters cannot be specifically measured, although it is often reported like that. Another in vivo technique is intracerebral microdialysis (de Lange et al., 2017). This technique is minimally invasive and its use in humans is therefore highly restricted, but can be used in animals to provide highly valuable data. It uses a probe being implanted into a selected location in the brain that has a semipermeable membrane by which molecules small enough to pass the membrane can be taken with the perfusion fluid.

* Corresponding author at: LACDR/Systems Biomedicine and Pharmacology, Leiden University, Einsteinweg 55, 2333 CC Leiden, the Netherlands.
E-mail address: ecmdelange@lacdr.leidenuniv.nl (E.C.M. De Lange).

https://doi.org/10.1016/j.ejps.2018.08.022
Received 27 May 2018; Received in revised form 14 August 2018; Accepted 15 August 2018
Available online 23 August 2018

Table 1
Different sites of kainite injections to induce Status Epilepticus (SE) in rats (intraperitoneal (IP) or intra-hippocampal (IH), and the number of rats included to determine brain capillary P-gp protein expression, and BBB P-gp mediated transport at the different days post SE.

Description	Group A	Group B	Group C
	IP kainate treatment	Microdialysis surgery followed by unilateral IH kainate treatment	Microdialysis surgery followed by unilateral IH kainate treatment and bilateral microdialysis experiments
Description for number or rats (n)			
Total of control rats and all kainate-treated rats	n = 40	n = 17	n = 35
Kainate-treated rats that reached scale IV or V seizures and were included in the P-gp expression analysis	n = 34	n = 13	n = 31
Euthanasia (days after control-treatment)	Day 1 (n = 1), day 2 (n = 1), 4 (n = 1), day 7 (n = 1), day 10 (n = 1), day 14 (n = 1), day 21 (n = 1), day 28 (n = 1) Total n = 8.	Day 2 (n = 1),day 7 (n = 1), day 22 (n = 1), Total n = 3	Day 2 (n = 1),day 7 (n = 1), day 22 (n = 1), Total n = 3
Euthanasia (days after kainate-treatment)	Day 1 (n = 3); day 2 (n = 5); day 3 (n = 1); day 4 (n = 2); day 7 (n = 5); day 10 (n = 2); 14 (n = 4); day 21 (n = 2), day 28 (n = 2) Total n = 26	Day 2 (n = 4), day 7 (n = 5), day 22 (n = 4), Total n = 13	Day 2 (n = 1), day 3 (n = 1), day 4 (n = 1), day 5 (n = 1), day 6 (n = 2), day 7 (n = 1), day 9 (n = 1), day 10 (n = 1), day 11 (n = 1), day 12 (n = 1), day 13 (n = 1), day 14 (n = 1), day 15 (n = 1), day 16 (n = 1), day 18 (n = 1), day 20 (n = 1), day 21 (n = 1), day 22 (n = 1), day 23 (n = 1), day 24 (n = 1), day 25 (n = 1), day 26 (n = 1, day 27 (n = 1), day 28 (n = 1), day 30 (n = 1), day 31 (n = 1), day 32 (n = 1), day 33 (n = 1), day 34 (n = 1), day 36 (n = 1). Total n = 31
Euthanasia (days after kainite treatment for rats that had successful microdialysis experiments)			day 2 (n = 1), day 3 (n = 1), day 4 (n = 1), day 5 (n = 1), day 6 (n = 2), day 7 (n = 1), day 9 (n = 1), day 10 (n = 1), day 12 (n = 1), day 13 (n = 1), day 14 (n = 1), day 16 (n = 1), day 22 (n = 1), day 25 (n = 1), day 27 (n = 1), day 30 (n = 1), day 32 (n = 1), day 34 (n = 1). Total n = 19

The fluid can be collected in intervals, and these samples can be analyzed on its drug content. It thereby provides unbound drug concentration-time profiles that can be related to unbound plasma concentration-time profiles to give BBB specific information on rate and extent of BBB transport, including active transporter functionality. (Westerhout et al., 2013).

One of the important brain diseases that has been associated with changes in P-gp functionality is pharmacoresistant epilepsy, as in epileptogenic brain tissue of patients with pharmacoresistant epilepsy, an increased expression of P-glycoprotein (P-gp) at the BBB has been found (Dombrowski et al., 2001; Marchi et al., 2016, 2004; Tishler et al., 1995). To investigate the potential role of P-gp in pharmacoresistant epilepsy, animals models that make use of induced kainite, pilocarpine, or electrically induced Status Epilepticus (SE) have been frequently employed, measuring P-gp gene mRNA expression and/or P-gp protein expression, and variable results on post-SE changes in P-gp expression at 24 h, 48 h, 7 days and/or 14 days post SE have been reported (Bankstahl and Löscher, 2008; Kuteykin-Teplyakov et al., 2009; Seegers et al., 2002; Van Vliet et al., 2004; Volk and Loscher, 2005; Volk et al., 2004).

To assess P-gp functionality, Syvänen et al. studied potential changes in BBB P-gp function in kainate induced SE rats, 7 days post SE, using PET experiments with (*R*)- C-11 Verapamil, and microdialysis experiments with quinidine, and BBB P-gp expression by immunohistochemistry in brain capillaries at 7 days post-SE (Syvänen et al., 2011; Syvänen et al., 2012b). These studies did not reveal any significant difference in brain P-gp function nor expression at 7 days post-SE compared to saline-treated (control) animals at this time point.

Taken together, studies on the relationship between time after SE, P-gp expression at the BBB and P-gp function at the BBB are inconsistent. The variable results may have been caused by differences in the methods used to induce SE, differences in protocols to measure P-gp expression, different techniques used to determine P-gp function, and inter-individual variability in severity of subsequent development of spontaneous seizures. Therefore it is of interest to investigate the time-course of P-gp expression following SE, in conjunction with BBB P-gp function.

In this study SE was induced in rats either using the intraperitoneal or intrahippocampal injection of kainite. The time-course of hippocampal brain capillary P-gp protein expression was assessed by immunohistochemistry. Changes in P-gp expression following intrahippocampal injection of kainite induced SE were most pronounced and related to changes in BBB hippocampal P-gp function in the same individual rats by intracerebral microdialysis using quinidine and mathematical modeling, for a period up to 5 weeks post SE. Data were analyzed by Non-linear Mixed Effect modeling (NONMEM), and the relation between brain capillary P-gp expression and P-gp functionality was assessed.

2. Methods

2.1. Animals

Adult male Sprague-Dawley rats (Harlan, Horst, The Netherlands) weighing 200–249 g on arrival were used throughout the study. After arrival, all animals were housed in groups of 5 to 6 per Makrolon type three cage for 7–14 days (Animal Facilities, Gorlaeus Laboratories, Leiden, the Netherlands) prior to the start of experiments. They were kept under standard environmental conditions (ambient temperature 21 ± 1 °C; humidity 60%; 12/12 h light/dark cycle in which white lights were switched on at 8:00 AM, in the presence of background noise, and undergoing daily handling), with ad libitum access to food (RM3 (E) DU, Special Diets Services B.V., Witham, Essex, England) and acidified water.

Between surgery and experiments, the animals were kept individually in cages for 7 days to recover from the surgical procedures. Animal procedures were performed in accordance with Dutch laws on animal experimentation. All experiments were approved by the Ethics Committee for Animal Experiments of Leiden University (approval numbers UDEC08180 and UDEC10057).

2.2. Experimental Study Designs

Table 1 shows the different sites of kainite injections to induce Status Epilepticus (SE) in rats (intraperitoneal (IP) or intra-hippocampal (IH), and the number of rats included to determine brain capillary P-gp protein expression and BBB P-gp mediated transport at the different days post SE.

2.2.1. Intraperitoneal (IP) Kainate Treatment (Group A)

Kainic acid (Sigma-Aldrich, Zwijndrecht, the Netherlands) was dissolved in saline and administered as repetitive intraperitoneal (IP mode) injections to rats until full-blown seizures were observed. First, an initial IP kainate dose of 10 mg/kg (2 mL/kg, in saline) was administered followed by 5 mg/kg (1 mL/kg) IP every 30–60 min until stage IV or V seizures according to Racine's scale occurred. (Racine, 1972), or when a total amount of 30 mg/kg kainate was reached. Vehicle, i.e. saline only, was administered IP to 8 control rats.

Most rats treated with IP injections of kainate displayed stage IV or V seizures (26 out of 32 rats, Table 1, Group A). Typically three kainate injections were needed, i.e. 20 mg/kg and SE was usually reached within 20 min after the last injection. Rats usually displayed seizures for 1–2 h. The seizures were not interrupted by any anti-epileptic drug. The rats that did not reach stage IV were discarded (n = 3), and some rats did not recover (n = 3). Two rats died as a result of the kainate treatment and one animal was taken out of the experiment and euthanized as it did not recover properly from the treatment. All other rats were included in the P-gp expression analysis. Rats were observed daily after treatment to monitor their recovery and development of spontaneous seizures. The IP treated rats, were euthanized by decapitation between 1 and 28 days after SE.

2.2.2. Unilateral Intrahippocampal (IH) Kainate Treatment (Group B)

In another group of rats intrahippocampal injection of kainate was performed.

Before surgery each rat received a subcutaneous injection (0.1 mL) of both the antibiotic Ampicillan 20% (Alfasan Nederland B.V. Woerden) and the analgesic Temgesic 0.3 mg/mL (Schering-Plough, Utrecht). All cannulas and electrodes that were to be implanted had undergone 24-h decontamination before use and during surgery eye cream was applied to the eyes to prevent dehydration.

2.2.2.1. Surgery. Each rat was anaesthetized with isoflurane (Pharmachemie BV, Haarlem, The Netherlands), and the animals' core temperature was maintained at 37 °C. The rats were placed in a stereotaxic frame. An incision on the top of the head was made using a scalpel. The skin was retracted and lidocaine was applied to the skull that was scraped, cleaned, and allowed to dry. Two small holes were drilled into the skull for insertion of the microdialysis guides (CMA/Microdialysis AB, Stockholm, Sweden) at the following co-ordinates relative to bregma: AP -5.6, L 4.6 and L - 4.6. Three additional holes were drilled for support screws as anchor points for the cement. The guides with dummy probes were inserted into the brain to a depth of −5.2 mm and fixed to the skull using dental cement.

2.2.2.2. Unilateral Intrahippocampal Kainate Treatment. After one week of recovery, the dummy probe was removed from the guide cannula and a customized injection probe, consisting of a modified CMA12 probe (CMA, Solna, Sweden with the tip cut by a laser to a length of 0.50 mm and a OD of 0.030 mm, was inserted. Kainic acid was dissolved (2 μg/μL) in minimal microdialysis perfusion solution (mPF; containing 140.3 mM sodium, 2.7 mM potassium, 1.2 mM calcium, 1.0 mM magnesium and 147.7 mM chloride) and injected to 46 rats, unilaterally into the left hippocampus (IH) via the modified CMA12 probe at a constant infusion of 0.1 μL/min for 10 min resulting in a total administered kainate dose of 1 μg. Vehicle, i.e. the minimal perfusion fluid, was administered according to the same procedure to control rats. The injection probe was carefully removed and replaced by the dummy probe approximately 20 min after stopping the kainate (n = 14) or vehicle (n = 2) infusion. Each animal was observed for at least 2 h after the start of the infusion to score the severity according to Racine's scale. Only the rats that reached scale IV or V seizures were included in the analysis, and one rat died.

To assess P-gp expression IH kainate treated rats were euthanized by decapitation, at day 2 (n = 4), 7 (n = 5) and 22 (n = 4) days after SE after kainate injection, and in total 3 for the controls at day 2 (n = 1), day 7 (n = 1) and day 22 (n = 1) (Table 1, Group B).

2.2.3. Unilateral Intrahippocampal (IH) Kainate Treatment (Group C)

In another group of rats the intrahippocampal (IH) injection of kainate was performed in the left hippocampus while the right hippocampus served as control. Bilateral microdialysis experiments were performed at 1–34 days post SE in individual rats.

2.2.3.1. Surgery. Each rat was anaesthetized with isoflurane (Pharmachemie BV, Haarlem, The Netherlands), and the animals' core temperature was maintained at 37 °C. The rats received two cannulas. To obtain blood samples, 3 cm of ID 0.28 mm cannula (SIMS Portex LTD, England) was inserted into the femoral artery, connected to 16 cm of ID 0.58 mm cannula (Portex Fine Bore polythene tubing Smiths Industries, Kent England).

For drug administration and blood sampling, 4 cm of ID 0.58 mm cannulas were inserted in the femoral vein and artery respectively, and connected to 16 cm of ID 0.58 mm cannula. Both cannulas were led subcutaneously to the back of the head where it was secured with a rubber ring. The cannulas were filled with FPEP to prevent clotting until the experiment.

Subsequently, the rats were placed in a stereotaxic frame and, like in group B, an incision on the top of the head was made using a scalpel. The skin was retracted and lidocaine was applied to the skull that was scraped, cleaned, and allowed to dry. Two small holes were drilled into the skull for insertion of the microdialysis guides (CMA/Microdialysis AB, Stockholm, Sweden) at the following co-ordinates relative to bregma: AP -5.6, L 4.6 and L - 4.6. Three additional holes were drilled for support screws as anchor points for the cement. The guides with dummy probes were inserted into the brain to a depth of −5.2 mm and fixed to the skull using dental cement.

2.2.3.2. Microdialysis Experiments. At 24 h before the start of the experiments the microdialysis dummies were replaced by microdialysis probes (CMA12). At the day of the experiment, the microdialysis tubing (1.2 μL/100 mm FEP-tubing CMA/Microdialysis AB, Stockholm, Sweden) was connected with tubing adapters (CMA/Microdialysis, Stockholm, Sweden) to the microdialysis probe's inlet and outlet. Microdialysis perfusion fluid was prepared according to Moghaddam et al. (Moghaddam and Bunney, 1989). Microdialysis vials were pre-weighed and placed in a cooled (4 °C) fraction collector (Univentor 820 Microsampler, Antec, Netherlands) to collect the microdialysate samples. Microdialysis probes were continuously flushed with mPF (2 μL/min, Bee-Hive, Bioanalytical Systems Inc. W-Lafayette, USA) and samples were collected before and during quinidine infusion: the first sample was taken 1 h prior to infusion of quinidine. Subsequently samples were collected at 20 min intervals at 1 h until 3 h after the start of quinidine infusion. After sample collection, vials were weighed to determine the actual probe perfusion rate. Sample series with regular perfusion rates between 1.9 and 2.1 μL/min (i.e. a maximal deviation of 5%) were included in data analysis. Samples were stored at −20 °C.

At $t = 0$ min the IV-infusion of quinidine (Sigma-Aldrich, Zwijndrecht, The Netherlands) was started according to a regimen to readily achieve plasma steady-state concentrations with the following infusion rates: From 0 to 25 min at 30 μL/min; from 25 to 60 min at 15 μL/min; and from 60 to 140 min at 10 μL/min, infused through the

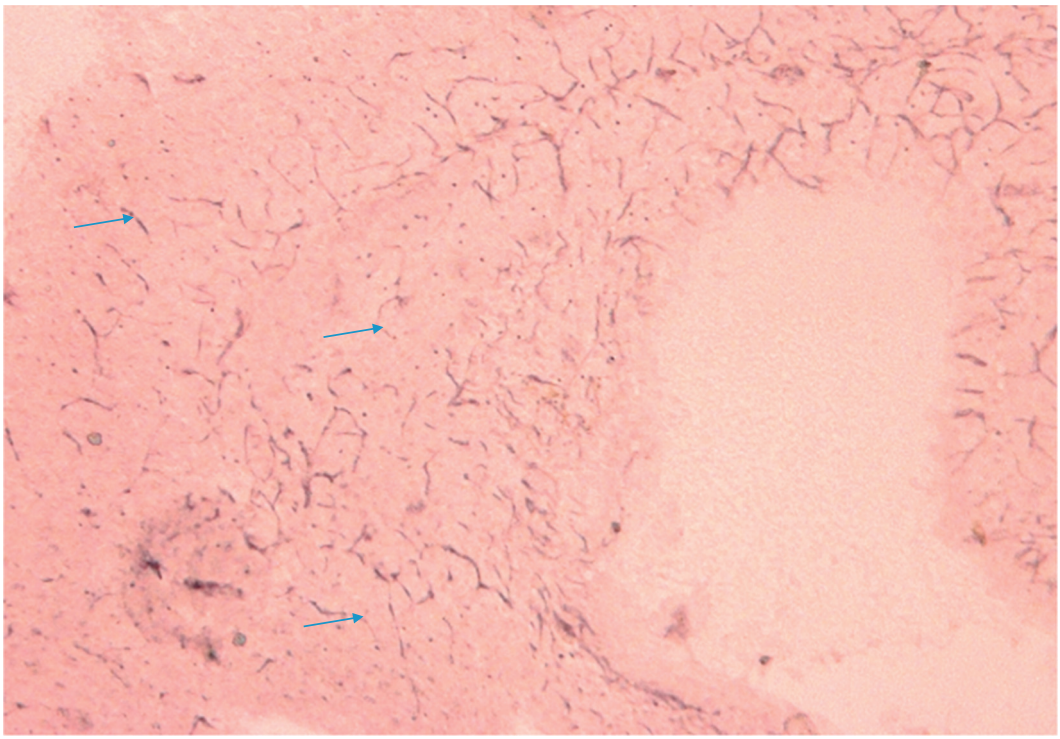

Fig. 1. Example of rat hippocampal brain capillary P-gp expression staining (50×).
Arrows serve as a few examples of this staining.

catheter in the femoral vein. On the basis of previous experiments (data not shown) at 140 min 90% of the steady-state concentration of quinidine was expected, and at that time 15 mg/kg Tariquidar (Xenova Group PLC, Cambridge, England, or API Services Inc. Westford, USA), was administered during 10 min. During the next 10 min the quinidine infusion was resumed, at a rate of 30 μL/min and from 160 min onwards it was 10 μL/min, to be stopped at 300 min. The total quinidine dose was 15 mg/kg/5 h.

During the experiment 10 blood samples of 200 μL were taken from the cannula in the femoral artery. The sampling was distributed over 7 h. The blood sample volume taken (200 μL) was replaced by the same volume of heparinized saline to sustain the circulating volume and to prevent clogging of the line.

At termination of the experiment the animals were euthanized with an intravenous overdose injection of Nembutal (1 mL). Following decapitation the brains were removed, rinsed, immediately embedded in Tissue-Tec (Sakura Finitek Europe, Zoeterwoude, The Netherlands) and snap frozen with liquid nitrogen to be stored at −80 °C.

2.3. Quantification of Quinidine in Plasma, Dialysates and Brain Tissue

For the HPLC analysis, quinidine was dissolved in methanol and diluted with water to a concentration of 100 μg/mL. This stock solution was further diluted in water (plasma and brain analysis) or perfusion fluid (microdialysate analysis) to construct calibration curves for quinidine analysis.

Quinidine was measured using HPLC with fluorescence detection. A LC10-ADVP HPLC pump (Shimadzu,'s-Hertogenbosch, the Netherlands) and an Altima C-18 150 × 4.6 mm column (Grace Altech, Breda, the Netherlands) was used. The mobile phase consisted of acetonitrile and phosphate buffer (25 mM) with triethyl-amine (10 mM) at a pH of 2.3 in a ratio of 17:83 (v/v) and 14/86 (v/v) for microdialysis and plasma samples, respectively, at a flow rate of 1 mL/min. Detection was performed using a Jasco FP-1920 fluorescence detector (Jasco, de Meern, the Netherlands) set at 488 nm for excitation and 512 nm for emission. Injection was performed using a Waters 717 autosampler (Waters, Etten-Leur, the Netherlands). The injection volume was 20 μL. Data acquisition was performed using Empower Software (Waters, Etten-Leur, the Netherlands).

Microdialysate was injected directly, without any pretreatment, and measured. For plasma analysis, 50 μL of the internal standard quinine (Sigma Aldrich, Zwijndrecht, the Netherlands) in a concentration of 500 ng/mL was added to 20 μL plasma sample. After homogenization with 200 μL of borate buffer pH 10, 5 mL of methyl tert-butyl ether was added. After vortexing, centrifugation, and freezing of the aqueous layer, the organic phase was evaporated to dryness. The extracts were reconstituted in 100 μL of mobile phase and centrifuged at 4000 × *g* during 5 min. The clean plasma extracts were injected using a mobile phase with an acetonitrile/buffer ratio of 1:6. Calibration was performed using 20 μL aliquots of quinidine in concentrations of 5, 10, 20, 50, 100, 200, 500, 1000, 2000 and 5000 ng/mL, which were added to 20 μL of blank plasma.

Variability (CV %) of the quantification of quinidine in plasma was below the 15% level. The precision and accuracy of quinidine measurements in microdialysates were < 10%. Limit of quantification was 5 ng/mL for plasma, 20 ng/mL for brain, and 1 ng/mL for microdialysate samples.

On the basis of microdialysis experimental quality criteria (perfusion flow deviation not larger than 5% from the intended 2 μL/min) and analytical criteria (blank microdialysis concentrations < 0.1 ng/ml), 14 rats were excluded from data analysis.

In vivo recovery was determined by retrodialysis (in vivo loss) and was found to be 24 ± 5.8%, independent of quinidine concentration and tariquidar treatment (Syvänen et al., 2012b). It was assumed that in vivo loss would equal in vivo gain. All microdialysis data were corrected for in vivo recovery to estimate brain extracellular fluid (brainECF) concentrations.

2.4. Immunohistology

2.4.1. Brain Capillary P-gp Protein Expression Staining in Brain Slices

A Leica CM 1900 cryostat, at a temperature between −16 and − 18 °C, was used to slice the brains into coronal 30 µm sections. Series of 6 slices were mounted on SuperFrostPlus glass slides capturing −2.56 mm, −3.14 mm, −3.30 mm, −3.60 mm, −3.80 mm, −4.30 mm relative to bregma respectively per brain and stored at −20 °C.

A immunohistochemistry staining protocol based on the use of 3,3-diaminobenzidine as chromogen to specifically stain brain capillary P-gp was applied, and P-gp expression was quantified as P-gp labelled area as previously published (Volk and Loscher, 2005; Syvänen et al., 2011; Syvänen et al., 2012b). In short, for each brain tissue slice the staining of P-gp protein was quantified in duplicate as & P-gp labelled area and these values were averaged per animal per slice location. Brain sections from all animals were stained simultaneously per group to obtain comparable staining. Fig. 1 shows an example of P-gp staining in brain capillaries.

2.5. Pharmacometric Analysis

Analysis of quinidine pharmacokinetic data as obtained in group C was performed using Nonlinear mixed-effects (NLME) modeling implemented in NONMEM VII (GloboMax LLC, Hanover, MD, USA). NLME modeling provides a good statistics-based solution for modeling data to a model that accounts for both fixed effects (group parameters assumed to be constant each time data is collected) and random effects (sample-dependent random variables). It is particularly useful in settings where repeated measurements are made on the same statistical units (longitudinal study), or where measurements are made on clusters of related statistical units. Because of their advantage in dealing with missing values, mixed effects models are often preferred over more traditional approaches such as repeated measures ANOVA.

2.5.1. Quinidine Pharmacokinetics in Plasma and Brain Extracellular Fluid

Quinidine pharmacokinetic (PK) profiles in plasma and brain extracellular fluid (brainECF), including inhibitory effect of tariquidar on P-gp transport function, was analyzed by systematic comparison of multiple possible PK models to find the model that described the obtained data best. Data from all rats were processed simultaneously. The subroutine ADVAN 6 and first-order conditional estimation with interaction were used throughout the modeling procedure. Model selection was based on the objective function value (OFV) with the lowest value corresponding to the best model. For nested models, OFV reductions of 3.83, 6.63 and 10.83 units correspond to improved fits at $p < 0.05$, $p < 0.01$ and $p < 0.001$ levels, respectively. Also, parameter estimates and their relative standard errors, residual error values, goodness-of-fit plots, and visually predictive check (VPC) were considered for model selection. During those analyses, software Xpose 4 (Jonsson and Karlsson, 1998). implemented in R 2.15.2 (The R foundation for Statistical Computing) accessed from Census (Wilkins, 2005) was used to assess the model performance. For example, predicted concentrations were plotted against measured concentrations and conditional weighted residuals (Hooker et al., 2007) were calculated and plotted against time and concentration.

The inter-individual variation of a parameter was described by the exponential variance model:

$$\theta_i = \theta_{pop} \cdot \exp(\eta_i) \quad (1)$$

where θ_i is the parameter in the i^{th} animal, θ_{pop} the parameter in a typical animal and η_i the inter-animal variability, which is assumed to be normally distributed around zero with a standard deviation ω. Eq. (2) provides a means to distinguish the parameter value for the i^{th} animal from the typical value predicted from the regression model. Inter-individual variation was investigated for all parameters, but incorporated only for those parameters for which it significantly improved the model ($p < 0.01$, OFV reduction of 6.63 units). Performance of the population pharmacokinetic model was evaluated using 500 additional bootstrap replicates (re-sampling with replacement) of the data by fitting the final model to them.

The pharmacokinetic (PK) quinidine model was constructed in two steps. In the first step, a PK model for quinidine plasma concentrations was developed. A two compartment model was chosen based on literature (Sugihara et al., 1993; Watari et al., 1989). Obtained plasma quinidine PK parameters were fixed, and then used for the analysis of brainECF quinidine concentrations as a second step. To describe the inhibitory effect of tariquidar on P-gp, plasma tariquidar PK was modeled assuming a one compartment model. Tariquidar plasma concentration data were taken from literature (Bankstahl and Löscher, 2008; Syvänen et al., 2011).

Obtained PK parameters of tariquidar (CL: 0.29 ± 0.024 L/h, V: 15 ± 0.18 L) were used to describe the inhibition of BBB P-gp function. For this calculation of tariquidar PK parameters, the pooled data method was applied since available plasma tariquidar PK data from literature were an average of pooled individual animals.

Afterwards, rat brain hemisphere (kainate versus vehicle treatment) and epilepsy severity stage IV or V, were defined as covariates to study their effects on the parameter estimates. Covariate analysis was performed based on the following equation;

$$\theta_i = \theta_{pop} \cdot \exp(\eta_i) \cdot \theta_{covar} \quad (2)$$

where θ_{COVAR} described the influence of kainate treatment or epilepsy stage on parameter estimate θ_{pop}. This model described the brain PK profile of quinidine including the data obtained during and after the start of the tariquidar infusion that led to inhibition of P-gp function at the BBB (CL31Pgp) well.

A stepwise forward addition and backward deletion approach was applied to test the significance ($p < 0.01$) for covariate inclusion. The residual variability was described with proportional error models for each compartment.

Ultimately, based on the above-mentioned criteria, the model displayed in Fig. S1 was able to describe the data best. In this model the influence of tariquidar on brainECF concentration of quinidine was described using an inhibitory indirect effect model as follows;

$$CL31Pgp(C_{TQD}) = CL31Pgp \cdot \left(1 - \frac{I_{max} \cdot C_{TQD}}{IC_{50} + C_{TQD}}\right) \quad (3)$$

where C_{TQD} indicates tariquidar plasma concentration and CL31Pgp (C_{TQD}) (or shortly CL31Pgp′) indicates P-gp mediated quinidine efflux transport (quinidine clearance) from brainECF to plasma in the presence of tariquidar, respectively. Maximal inhibition of P-gp by tariquidar (I_{max}) was set to 1. The concentration that would inhibit P-gp for 50% (IC_{50}) was taken form literature, (80 nM) (Mistry et al., 2001).

3. Results

3.1. Brain Capillary P-gp Expression

3.1.1. IP Kainate Treatment - Group A

It was found that the time course of changes in hippocampal brain capillary P-gp protein expression following SE by IP kainate (Fig. 2) showed an increase followed by a decrease. No difference between kainate and control rat hippocampus could be found.

3.1.2. IH Kainate Treatment- Group B

Of all rats of group B, brain capillary P-gp protein expression was investigated at 2 (n = 4), 7 (n = 5) and 22 days (n = 4) post IH kainate induced SE and controls at day 2 (n = 1), day 7 (n = 1) and day 22 (n = 1) (Fig. 3). P-gp expression had a pattern with increase followed by a decrease, similar to group A, but with higher values of P-gp

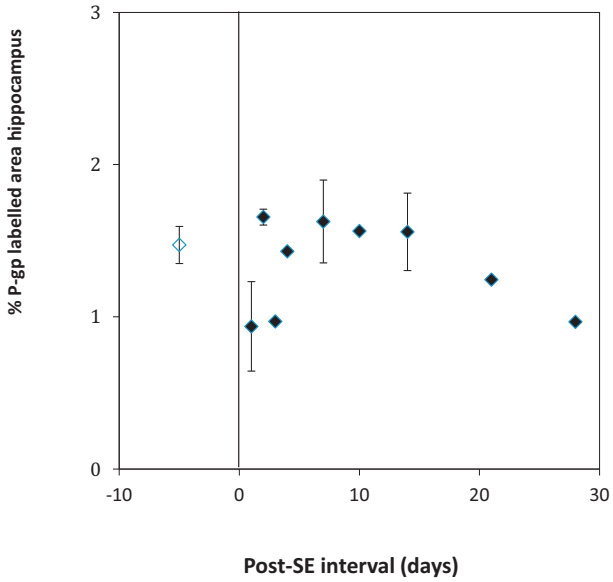

Fig. 2. Hippocampal brain capillary P-gp expression (% P-gp labelled area), in controls (at virtual time point −5 days) and IP kainite induced SE rats, at different post SE days.

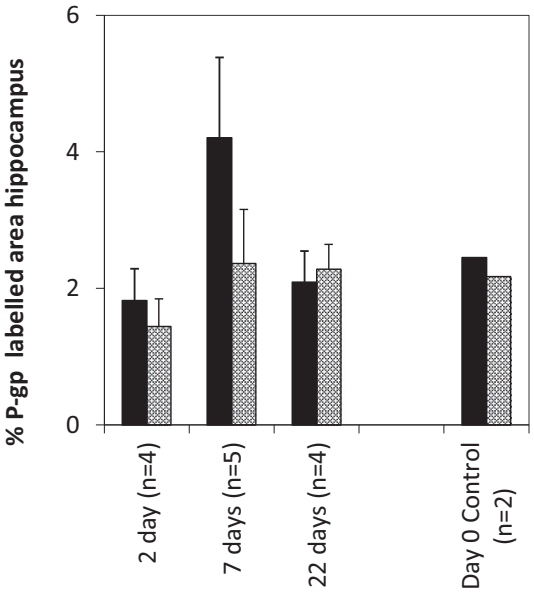

Fig. 3. Hippocampal brain capillary P-gp expression (% P-gp labelled area), in controls and IH kainate induced SE rats, at different post SE days.

expression. This trend was mostly pronounced for the kainate treated hippocampus. No such changes were seen in the controls. As the changes in brain capillary protein P-gp expression were higher in group B following IH compared to than in group A following IP kainate injection, IH kainite injection was considered best suited for further investigation on the time-course relation between BBB P-gp expression and BBB P-gp function using microdialysis.

3.1.3. IH Kainate Treatment and Microdialysis Experiments - Group C

Results of P-gp expression in the rats of group C are shown in Fig. 4. The brain capillary P-gp protein expression as a function of post SE days is shown for both left (kainate injection) and left (control injection) hippocampal areas. Brain capillary P-gp expression increased to maximum levels around 7–14 days and then declined over the next 3 weeks. In contrast to group B, in group C there was no significant difference in

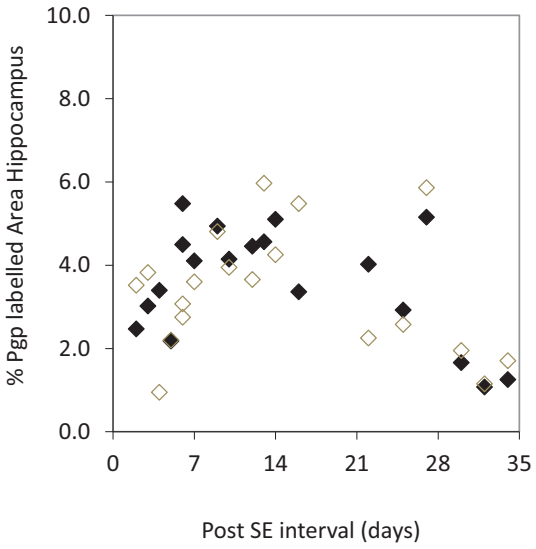

Fig. 4. Hippocampal brain capillary P-gp expression (% P-gp labelled area) in IH kainate induced SE in treated hippocampus (black diamonds) and control hippocampus (open diamonds) at different days following SE, of rats that underwent bilateral hippocampal microdialysis experiments.

brain capillary P-gp protein expression between the left and right hippocampus. This indicates that the presence of the microdialysis with induction of SE makes that brain capillary P-gp expression in both hippocampi show similar patterns. As differences levels of P-gp expressions were found over time, the comparison with BBB P-gp functionality could still be made.

3.2. Pharmacokinetics of Quinidine

3.2.1. Plasma Pharmacokinetics

Plasma concentrations of quinidine were obtained as a function of time (Fig. 5a). The infusion scheme used for the intravenous administration of quinidine led, within minutes, to concentrations very close to steady state, and TQD apparently did not affect the plasma concentrations of quinidine.

3.2.2. Bilateral Hippocampal Microdialysis

In parallel to the serial blood sampling, bilateral microdialysis sampling was performed. Microdialysis data were obtained from both the left (kainate treated) and right (control treated) hemisphere. The quinidine brainECF concentration-time profiles are shown in Fig. 5b. No differences in quinidine brainECF concentrations were found between kainate treated and control hippocampus. Upon administration of tariquidar, a substantial increase in the brainECF quinidine concentrations in both hippocampi was observed, indicating successful blocking of BBB P-gp functionality, i.e. a decrease in P-gp mediated efflux of quinidine.

3.3. Pharmacometric Analysis of BBB P-gp Expression & P-gp Functionality

3.3.1. P-gp Mediated Transport at the BBB

Plasma and brainECF PK profiles of quinidine, respectively before and after tariquidar administration (Fig. 5), were described well by the proposed quinidine brain distribution model (Fig. S1). The resulting model parameters are shown in Table 2, together with their inter-individual variability (η) and residual error. For the brainECF PK of quinidine (Fig. 5), covariate analysis did not reveal a difference between kainate-treated and control hippocampus. However, a clear influence of P-gp blockage by tariquidar was demonstrated.

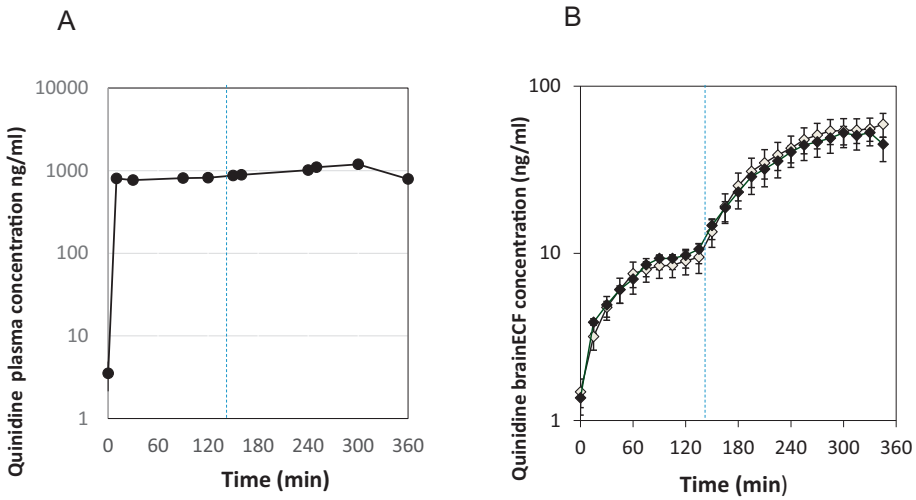

Fig. 5. Pharmacokinetics of quinidine in A) plasma and B) brainECF of kainate treated hippocampus (black diamonds) and control hippocampus (open diamonds). Quinidine was administered as a combination of a fast and slow infusion (see Material and Methods), and tariquidar was administered around 110 min.

3.3.2. Relationship Between P-gp Expression and P-gp Functionality

For the purpose of the present study, the differences in brain capillary P-gp protein expression between individual animals at different time points after SE were sufficiently large to establish whether there a correlation would exist between brain capillary P-gp protein expression and function. Individual estimates of P-gp function at the BBB (CL31Pgp) were based on the microdialysis and plasma data of each individual rat in absence (CLP31gp) and presence of the P-gp inhibitor tariquidar (CL31Pgp′). P-gp expression was measured ex-vivo in the same rat. The individual corresponding values for brain capillary P-gp protein expression and function for each rat are shown in Fig. 6. No correlation between these two parameters was observed.

Table 2
Pharmacokinetic modeling parameter values. Results of NLME modeling of pharmacokinetic data obtained for group C. Parameter estimates of plasma and brain pharmacokinetics of quinidine from the original dataset and from 500 bootstrap replicates. CL1, Q2, CL13, CL31Pgp, and CL31 are the clearances from plasma, intercompartmental clearance between central and peripheral compartment, passive transport from plasma to brain, P-gp mediated transport from brain to plasma, and passive transport from brain to plasma, respectively. V1, V2, and V3 are the volume of distribution in central plasma, peripheral tissue, and brain ECF. V3 was fixed to its physiological volume (145 µL for each left and right brain ECF; Westerhout et al., 2012). Tariquidar plasma pharmacokinetics is described by CL5 (clearance from plasma) and V5 (central volume of distribution).

	Original mean	SE	Bootstrap median	Percentile 2.5%	Percentile 95%
Parameter values					
Cl1 (L/H)	3.68	0.56	3.45	0.56	4.46
V1 (L)	0.19	0.06	0.21	0.08	0.39
Q2 (L/H)	22.3	4.9	20.9	12.1	34.7
V2 (L)	12.5	1.9	13.0	9.9	29.1
CL13 (µL/H)	8.2	1.8	8.0	5.4	11.8
CL31Pgp (µL/H)	29.1	6.5	27.9	17.5	41.7
CL31 (µL/H)	7.6	2.2	7.2	3.7	12.1
Imax	1	Fix			
V3 (mL)	0.145	Fix			
IC50 (ng/ML)	25	Fix			
V5 (L)	15	Fix			
Cl5 (L/H)	0.29	Fix			
Inter-individual variability					
CL1	0.419	0.214	0.405	0.10	3.42
Q2	0.410	0.252	0.466	0.084	1.20
CL13Pgp	0.45	0.11	0.45	0.25	0.66
CL31	0.94	0.37	0.96	0.39	1.88
Residual error					
CMT1 PROP	0.098	0.024	0.095	0.055	0.154
CMT3 KA + PROP	0.108	0.045	0.109	0.034	0.227
CMT4 KA- PROP	0.148	0.073	0.144	0.039	0.501

4. Discussion

A proper understanding of P-gp mediated transport (functionality) at the BBB is needed to interpret, understand and predict pharmacokinetic (PK)- pharmacodynamics (PD) relationships CNS drugs that are substrates of P-gp, especially since P-gp functionality may be different in different conditions. (de Lange et al., 2017). An important condition in which potential changes in P-gp functionality may occur is pharmacoresistant epilepsy, and many investigations have used rat Status Epilepticus (SE) models of temporal lobe epilepsy to investigate such

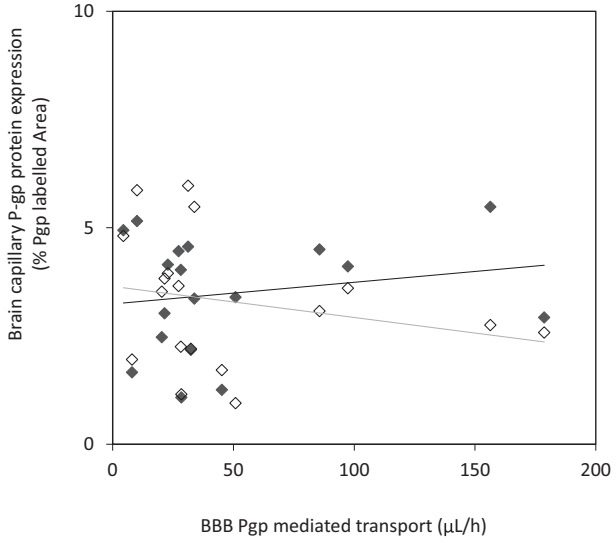

Fig. 6. BBB P-gp expression (% P-gp labelled area) versus BBB P-gp function (CL31Pgp) for each individual rat of group C. Black diamonds = kainate treated hippocampus, open diamonds = control hippocampus. The trendlines indicate a lack of correlation.

potential changes in which often P-gp expression (mRNA, protein) has been used as a biomarker of P-gp transporter functionality. However, data on P-gp expression and P-gp function that have been reported, were not directly comparable, as different SE models, different timings after SE, and different techniques were used.

In the present investigation the relation between brain capillary P-gp expression and P-gp mediated transport at the BBB was investigated in the same animal, and no such relationship was found.

4.1. Brain Capillary P-gp Expression

P-gp expression at the BBB was investigated over a period of ~5 weeks post SE, induced following IP administration of kainate (**group A**) or IH administration (**group B and C**). In all groups brain capillary P-gp protein expression changed over time, which was most pronounced after IH administration of kainate (**group B**). In group B differences were found between P-gp expression at the treated and nontreated side at day 7, while in group C (with microdialysis) no time-dependent differences were found; both hippocampi showed changes in P-gp expression. This indicated that the control hippocampus in an individual rat could not serve as the side where no changes in P-gp expression would occur. However, the relation between P-gp expression and P-gp functionality could still be investigated.

4.2. P-gp Mediated Transport (P-gp Functionality) at the BBB

Changes in brain capillary P-gp protein expression were the highest in the IH treated rats (**group B**) and this model was therefore best suited to assess the relationship between P-gp expression and functionality, the latter by using quinidine BBB transport in absence and presence of tariquidar (**group C**). At different days after induction on SE, bilateral microdialysis experiments using were performed in the kainate treated and control hippocampus of individual rats. It was found that quinidine brainECF concentrations were similar in both hippocampi. Blockage of P-gp by tariquidar led to a substantial (~5-fold) increase in brainECF quinidine concentrations, in both hippocampal brain regions. P-gp mediated efflux transport was calculated using a mathematical model of quinidine brain distribution with tariquidar co-administration as a covariate.

4.3. Relationship Between P-gp Expression and P-gp Functionality

As brain capillary P-gp protein expression was assessed after the microdialysis experiments, a direct relationship between P-gp expression and mediated transport at the BBB could be directly investigated for each individual rat. We used well-established techniques and protocols for determining BBB specific P-gp expression (Volk and Loscher, 2005; Syvänen et al., 2011) and BBB specific P-gp function (Syvänen et al., 2012a, 2012b; Westerhout et al., 2013). Also, it has been shown that BBB transport of quinidine decreases when P-gp is upregulated (Chan et al., 2013).

This leaves the lack between BBB P-gp expression and function as demonstrated in this study to be compared with apparent contradicting findings reported in literature (Bauer et al., 2014; Feldmann et al., 2013; Jing et al., 2010; Micuda et al., 2008; Ransohoff et al., 2007; Uchida et al., 2014). In different pharmacoresistant epilepsy rat models, radioactive labelled P-gp substrates were used as a PET ligands ([^{11}C] verapamil and [^{11}C]quinidine as strong P-gp substrates, and [^{11}C]flumazenil and 5HT$_{1A}$-receptor antagonist [^{18}F]MPPF as weak P-gp substrates (Bankstahl et al., 2011; Bartmann et al., 2010; Syvänen et al., 2011; Syvänen et al., 2012a; Syvänen et al., 2013). Most of these studies have shown differences in P-gp function between post SE rats and controls in brain distribution of these PET ligands (Bankstahl et al., 2011; Syvänen et al., 2011; Syvänen et al., 2013; Bartmann et al., 2010; Syvänen et al., 2012a; Müllauer et al., 2012) including the effect of P-gp inhibition.

However, PET measurements reflect tracer activities, which (at best) reflect total brain concentrations of the tracer. Because BBB transport is driven by the difference in the unbound concentrations at either side of the BBB (De Lange et al., 1997; Hammarlund-Udenaes et al., 1997) it is impossible to determine BBB specific transport and therewith BBB specific P-gp function by PET. So, a difference in total brain activity of a P-gp substrate tracer between kainate and control rats detected by PET may not necessarily indicate changes in BBB P-gp, because it can also reflect changes in intra-brain distribution by changes in P-gp at the level of brain cells that may occur as well (Gibson et al., 2012; Lee et al., 2001; Ronaldson et al., 2008; Zhang et al., 1999). This has been demonstrated in a microdialysis study by Syvänen et al.; in this study, pre-administration of tariquidar resulted in an 7.2 fold increase of brainECF concentrations of quinidine, while total brain concentrations increased 40-fold, 7 days post SE induction by kainate (Syvänen et al., 2012b). Thus, as PET studies cannot discriminate between changes in P-gp function at the BBB and that at the level of brain cells, our data are not in contrast with these previous findings per se, as we have specifically measured P-gp function at the BBB level.

Then, in another study by van Vliet et al., P-gp expression in brains of post-SE rats was found to be 2-fold and 1,5 fold higher in the temporal hippocampus and para-hippocampal cortex, respectively, with corresponding total brain phenytoin concentrations being decreased by 30% and 20% (van Vliet et al., 2007). As in this study total brain concentrations were measured, it cannot be concluded that lowered brain concentrations of phenytoin resulted from increased BBB P-gp functionality, as this was not measured, while also P-gp expression and functionality measurements used in this study were not specific for BBB.

Finally, in an elegant study of Uchida et al., reconstructed P-gp/mdr1a functions were integrated with unbound fractions of verapamil in plasma and brain to reconstruct brain distribution (total brain-plasma concentration ratio, Kp) for a variety of epilepsy mice models (Uchida et al., 2014). In that manner they found that reconstructed Kpuu brain values for verapamil were changed in the different mice models of epilepsy. It should be noted however, that these studies used isolated brain capillaries for determining the P-gp protein expression in brain capillaries. Furthermore, the unbound brain concentrations were estimated indirectly by the brain slide method, as naïve brain slices of the different mice epilepsy models incubated with verapamil for 6 h. In our study we assessed P-gp functionality in vivo, with individual rat P-gp expression as obtained within the same hippocampus. Thus, it seems that the existence of a relation between BBB P-gp expression and functionality is as least depending on the methodologies used.

4.4. Concluding Remarks

It should be realized that we need specific data for a proper understanding of P-gp mediated transport (functionality) at the BBB and beyond, to understand and predict pharmacokinetic (PK)- pharmacodynamic (PD) relationships of CNS drugs that are substrates of P-gp, especially since changes in P-gp functionality may be observed in disease conditions, and may also be brain location dependent.

While many studies report on P-gp expression/functionality at the BBB, in the majority of those, no explicit distinction is made between P-gp expression or functionality at the level of the BBB and those at the level of the brain parenchymal cells. In the current study the direct in vivo relationship between brain capillary P-gp protein expression and functionality in epileptic kainate treated and control rats was studied directly, within the same animal, and no such relationship was found. Therefore, it seems that brain capillary P-gp functionality does not necessarily reflect BBB P-gp expression. The study of Uchida et al. was the only study in which BBB specific P-gp expression and functionality was investigated and their conclusion was that p-gp expression and P-gp functionality at the BBB was related (Uchida et al., 2014). Thus, the existence or absence of such relationship seems to depend at least on

methodologies used, and on the animal and type of model that has been used to investigate such relationships. Altogether, it warrants a critical view on the interpretation of reported changes in (supposedly) BBB P-gp expression as a biomarker of P-gp functionality.

Supplementary data to this article can be found online at https://doi.org/10.1016/j.ejps.2018.08.022.

Competing Interests

None of the authors has any competing interests.

Acknowledgements

This manuscript deals with combining microdialysis experimental data and advanced mathematical modeling and is dedicated to Prof Dr Hartmut Derendorf, who is an expert in microdialysis, and pharmacokinetic/pharmacodynamic modeling.

Furthermore, the authors are grateful for the financial support of Foundation Epilepsy Institutions the Netherlands (SEIN) and the EU 7th Framework Programme EURIPIDES (FP7-under grant agreement n° 201380), and the PKPD modeling platform 2 (2012–2017). Finally, the work of Dr. N. Doorenweert and Dr. M. Labots for executing the microdialysis experiments, and P-gp staining, is highly appreciated.

References

Bankstahl, J.P., Löscher, W., 2008. Resistance to antiepileptic drugs and expression of P-glycoprotein in two rat models of status epilepticus. Epilepsy Res. 82, 72–87. https://doi.org/10.1016/j.eplepsyres.2008.07.007.

Bankstahl, J.P., Bankstahl, M., Kuntner, C., Stanek, J., Wanek, T., Meier, M., Ding, X.-Q., Muller, M., Langer, O., Loscher, W., 2011. A novel positron emission tomography imaging protocol identifies seizure-induced regional overactivity of P-glycoprotein at the blood-brain barrier. J. Neurosci. 31, 8803–8811. https://doi.org/10.1523/JNEUROSCI.6616-10.2011.

Bartmann, H., Fuest, C., La Fougere, C., Xiong, G., Just, T., Schlichtiger, J., Winter, P., Böning, G., Wängler, B., Pekcec, A., Soerensen, J., Bartenstein, P., Cumming, P., Potschka, H., 2010. Imaging of P-glycoprotein-mediated pharmacoresistance in the hippocampus: proof-of-concept in a chronic rat model of temporal lobe epilepsy. Epilepsia 51, 1780–1790. https://doi.org/10.1111/j.1528-1167.2010.02671.x.

Bauer, M., Karch, R., Zeitlinger, M., Liu, J., Koepp, M.J., Asselin, M.C., Sisodiya, S.M., Hainfellner, J.A., Wadsak, W., Mitterhauser, M., Müller, M., Pataraia, E., Langer, O., 2014. In vivo P-glycoprotein function before and after epilepsy surgery. Neurology 83, 1326–1331. https://doi.org/10.1212/WNL.0000000000000858.

Chan, G.N.Y., Patel, R., Cummins, C.L., Bendayan, R., 2013. Induction of P-glycoprotein by antiretroviral drugs in human brain microvessel endothelial cells. Antimicrob. Agents Chemother. 57, 4481–4488. https://doi.org/10.1128/AAC.00486-13.

De Lange, E.C.M., Danhof, M., De Boer, A.G., Breimer, D.D., 1997. Methodological considerations of intracerebral microdialysis in pharmacokinetic studies on drug transport across the blood-brain barrier. Brain Res. Rev. 25. https://doi.org/10.1016/S0165-0173(97)00014-3.

de Lange, E.C.M., van den Brink, W., Yamamoto, Y., de Witte, W.E.A., Wong, Y.C., 2017. Novel CNS drug discovery and development approach: model-based integration to predict neuro-pharmacokinetics and pharmacodynamics. Expert Opin. Drug Discovery 1–12. https://doi.org/10.1080/17460441.2017.1380623.

Dombrowski, S.M., Desai, S.Y., Marroni, M., Cucullo, L., Goodrich, K., Bingaman, W., Mayberg, M.R., Bengez, L., Janigro, D., 2001. Overexpression of multiple drug resistance genes in endothelial cells from patients with refractory epilepsy. Epilepsia 42, 1501–1506. https://doi.org/10.1046/j.1528-1157.2001.12301.x.

Erdö, F., Denes, L., De Lange, E., 2017. Age-associated physiological and pathological changes at the blood-brain barrier: a review. J. Cereb. Blood Flow Metab. 37. https://doi.org/10.1177/0271678X16679420.

Feldmann, M., Asselin, M.-C., Liu, J., Wang, S., McMahon, A., Anton-Rodriguez, J., Walker, M., Symms, M., Brown, G., Hinz, R., Matthews, J., Bauer, M., Langer, O., Thom, M., Jones, T., Vollmar, C., Duncan, J.S., Sisodiya, S.M., Koepp, M.J., 2013. P-glycoprotein expression and function in patients with temporal lobe epilepsy: a case-control study. Lancet Neurol. 12, 777–785. https://doi.org/10.1016/S1474-4422(13)70109-1.

Gibson, C.J., Hossain, M.M., Richardson, J.R., Aleksunes, L.M., 2012. Inflammatory regulation of ATP binding cassette efflux transporter expression and function in microglia. J. Pharmacol. Exp. Ther. 343, 650–660. https://doi.org/10.1124/jpet.112.196543.

Hammarlund-Udenaes, M., Paalzow, L.K., De Lange, E.C.M., 1997. Drug equilibration across the blood-brain barrier - pharmacokinetic considerations based on the microdialysis method. Pharm. Res. 14. https://doi.org/10.1023/A:1012080106490.

Hooker, A.C., Staatz, C.E., Karlsson, M.O., 2007. Conditional weighted residuals (CWRES): a model diagnostic for the FOCE method. Pharm. Res. 24, 2187–2197. https://doi.org/10.1007/s11095-007-9361-x.

Jing, X., Liu, X.X., Wen, T., Xie, S., Yao, D., Liu, X.X., Wang, G., Xie, L., 2010. Combined effects of epileptic seizure and phenobarbital induced overexpression of P-glycoprotein in brain of chemically kindled rats: research paper. Br. J. Pharmacol. 159, 1511–1522. https://doi.org/10.1111/j.1476-5381.2009.00634.x.

Jonsson, E.N., Karlsson, M.O., 1998. Xpose - An S-PLUS based population pharmacokinetic/pharmacodynamic model building aid for NONMEM. Comput. Methods Prog. Biomed. 58, 51–64. https://doi.org/10.1016/S0169-2607(98)00067-4.

Kervezee, L., Hartman, R., Van Den Berg, D.-J., Shimizu, S., Emoto-Yamamoto, Y., Meijer, J.H., De Lange, E.C.M., 2014. Diurnal variation in P-glycoprotein-mediated transport and cerebrospinal fluid turnover in the brain. AAPS J. 16. https://doi.org/10.1208/s12248-014-9625-4.

Kuteykin-Teplyakov, K., Brandt, C., Hoffmann, K., Löscher, W., 2009. Complex time-dependent alterations in the brain expression of different drug efflux transporter genes after status epilepticus. Epilepsia 50, 887–897. https://doi.org/10.1111/j.1528-1167.2008.01916.x.

Lee, G., Dallas, S., Hong, M., Bendayan, R., 2001. Drug transporters in the central nervous system: brain barriers and brain parenchyma considerations. Pharmacol. Rev. 53, 569–596 (https://doi.org/Animals Blood-Brain Barrier/*physiology Central Nervous System/*metabolism Humans Membrane Transport Proteins/*metabolism Neuroglia/metabolism Neurons/metabolism Pharmaceutical Preparations/*metabolism Research Support, Non-U.S. Gov't).

Marchi, N., Hallene, K.L., Kight, K.M., Cucullo, L., Moddel, G., Bingaman, W., Dini, G., Vezzani, A., Janigro, D., 2004. Significance of MDR1 and multiple drug resistance in refractory human epileptic brain. BMC Med. 2 (37). https://doi.org/10.1186/1741-7015-2-37.

Marchi, N., Banjara, M., Janigro, D., 2016. Blood – brain barrier, bulk flow, and interstitial clearance in epilepsy. J. Neurosci. Methods 260, 118–124. https://doi.org/10.1016/j.jneumeth.2015.06.011.

Micuda, S., Brcakova, E., Fuksa, L., Cermanova, J., Osterreicher, J., Hroch, M., Mokry, J., Pejchal, J., Martinkova, J., Staud, F., 2008. P-glycoprotein function and expression during obstructive cholestasis in rats. Eur. J. Gastroenterol. Hepatol. 20, 404–412. https://doi.org/10.1097/MEG.0b013e3282f471bf.

Mistry, P., Stewart, A.J., Dangerfield, W., Okiji, S., Liddle, C., Bootle, D., Plumb, J.A., Templeton, D., Charlton, P., 2001. In vitro and in vivo reversal of P-glycoprotein-mediated multidrug resistance by a novel potent modulator, XR9576. Cancer Res. 61 (2), 749–758.

Moghaddam, B., Bunney, B.S., 1989. Ionic composition of microdialysis perfusing solution alters the pharmacological responsiveness and basal outflow of striatal dopamine. J. Neurochem. 53, 652–654. https://doi.org/10.1111/j.1471-4159.1989.tb07383.x.

Müllauer, J., Kuntner, C., Bauer, M., Bankstahl, J.P., Müller, M., Voskuyl, R.A., Langer, O., Syvänen, S., 2012. Pharmacokinetic modeling of P-glycoprotein function at the rat and human blood-brain barriers studied with (R)-[11C]verapamil positron emission tomography. EJNMMI Res. 2, 1–15. https://doi.org/10.1186/2191-219X-2-58.

Racine, R.J., 1972. Modification of seizure activity by electrical stimulation: II. Motor seizure. Electroencephalogr. Clin. Neurophysiol. 32, 281–294. https://doi.org/10.1016/0013-4694(72)90177-0.

Ransohoff, R.M., Liu, L., Cardona, A.E., 2007. Chemokines and chemokine receptors: multipurpose players in neuroinflammation. Int. Rev. Neurobiol. 82, 187–204. https://doi.org/10.1016/S0074-7742(07)82010-1.

Ronaldson, P.T., Persidsky, Y., Bendayan, R., 2008. Regulation of ABC membrane transporters in glial cells: relevance to the pharmacotherapy of brain HIV-1 infection. Glia 56, 1711–1735. https://doi.org/10.1002/glia.20725.

Seegers, U., Potschka, H., Löscher, W., 2002. Transient increase of P-glycoprotein expression in endothelium and parenchyma of limbic brain regions in the kainate model of temporal lobe epilepsy. Epilepsy Res. 51, 257–268. https://doi.org/10.1016/S0920-1211(02)00156-0.

Sugihara, N., Furuno, K., Kita, N., Murakami, T., Yata, N., 1993. The influence of increased plasma protein binding on the disposition of quinidine in turpentine-treated rats. Biol. Pharm. Bull. 16, 63–67. https://doi.org/10.1248/bpb.16.63.

Syvänen, S., Luurtsema, G., Molthoff, C.F., Windhorst, A.D., Huisman, M.C., Lammertsma, A.A., Voskuyl, R.A., de Lange, E.C., 2011. (R)-[11C]verapamil PET studies to assess changes in P-glycoprotein expression and functionality in rat blood-brain barrier after exposure to kainate-induced status epilepticus. BMC Med. Imaging 11. https://doi.org/10.1186/1471-2342-11-1.

Syvänen, S., Labots, M., Tagawa, Y., Eriksson, J., Windhorst, A.D., Lammertsma, A.A., De Lange, E.C., Voskuyl, R.A., 2012a. Altered GABA(A) receptor density and unaltered blood brain barrier transport in a kainate model of epilepsy: an in vivo study using 11C-flumazenil and PET. J. Nucl. Med. 53 (12), 1974–1983. https://doi.org/10.2967/jnumed.112.104588.

Syvänen, S., Schenke, M., Van Den Berg, D.-J., Voskuyl, R.A., De Lange, E.C., 2012b. Alteration in P-glycoprotein functionality affects intrabrain distribution of quinidine more than brain entry-a study in rats subjected to status epilepticus by kainate. AAPS J. 14. https://doi.org/10.1208/s12248-011-9318-1.

Syvänen, S., Russmann, V., Verbeek, J., Eriksson, J., Labots, M., Zellinger, C., Seeger, N., Schuit, R., Rongen, M., van Kooij, R., Windhorst, A.D., Lammertsma, A.A., de Lange, E.C., Voskuyl, R.A., Koepp, M., Potschka, H., 2013. [11C]quinidine and [11C]laniquidar PET imaging in a chronic rodent epilepsy model: impact of epilepsy and drug-responsiveness. Nucl. Med. Biol. 40. https://doi.org/10.1016/j.nucmedbio.2013.05.008.

Tishler, D.M., Weinberg, K.I., Hinton, D.R., Barbaro, N., Annett, G.M., Raffel, C., 1995. MDR1 gene expression in brain of patients with medically intractable epilepsy. Epilepsia 36, 1–6. https://doi.org/10.1111/j.1528-1157.1995.tb01657.x.

Uchida, Y., Ohtsuki, S., Terasaki, T., 2014. Pharmacoproteomics-based reconstruction of in vivo P-glycoprotein function at blood-brain barrier and brain distribution of substrate verapamil in pentylenetetrazole-kindled epilepsy, spontaneous epilepsy, and phenytoin treatment models. Drug Metab. Dispos. 42, 1719–1726. https://doi.org/

10.1124/dmd.114.059055.
Van Vliet, E., Aronica, E., Redeker, S., Marchi, N., Rizzi, M., Vezzani, A., Gorter, J., 2004. Selective and persistent upregulation of mdr1b mRNA and P-glycoprotein in the parahippocampal cortex of chronic epileptic rats. Epilepsy Res. 60, 203–213. https://doi.org/10.1016/j.eplepsyres.2004.06.005.
van Vliet, E.A., van Schaik, R., Edelbroek, P.M., Voskuyl, R.A., Redeker, S., Aronica, E., Wadman, W.J., Gorter, J.A., 2007. Region-specific overexpression of P-glycoprotein at the blood-brain barrier affects brain uptake of phenytoin in epileptic rats. J. Pharmacol. Exp. Ther. 322, 141–147. https://doi.org/10.1124/jpet.107.121178.
Volk, H.A., Loscher, W., **2005**. Multidrug resistance in epilepsy: rats with drug-resistant seizures exhibit enhanced brain expression of P-glycoprotein compared with rats with drug-responsive seizures. Brain 128, 1358–1368.
Volk, H.A., Burkhardt, K., Potschka, H., Chen, J., Becker, A., Löscher, W., 2004. Neuronal expression of the drug efflux transporter P-glycoprotein in the rat hippocampus after limbic seizures. Neuroscience 123 (3), 751–759. https://doi.org/10.1016/j.neuroscience.2003.10.012.
Watari, N., Wakamatsu, A., Kaneniwa, N., 1989. Comparison of disposition parameters of quinidine and quinine in the rat. Aust. J. Pharm. 12, 608–615. https://doi.org/10.1248/bpb1978.12.608.
Westerhout, J., Ploeger, B., Smeets, J., Danhof, M., Lange, E.C.M., 2012. Physiologically-based pharmacokinetic modeling to investigate regional brain distribution kinetics in rats. AAPS J. 14 (3), 543–553.
Westerhout, J., Smeets, J., Danhof, M., De Lange, E.C.M., 2013. The impact of P-gp functionality on non-steady state relationships between CSF and brain extracellular fluid. J. Pharmacokinet. Pharmacodyn. 40 (3), 327–342. https://doi.org/10.1007/s10928-013-9314-4.
Wilkins, J.J., 2005. NONMEMory: a run management tool for NONMEM. Comput. Methods Prog. Biomed. 78, 259–267. https://doi.org/10.1016/j.cmpb.2005.02.003.
Yamamoto, Y., Välitalo, P.A., Wong, Y.C., Huntjens, D.R., Proost, J.H., Vermeulen, A., Krauwinkel, W., Beukers, M.W., Kokki, H., Kokki, M., Danhof, M., van Hasselt, J.G.C., de Lange, E.C.M., 2018. Prediction of human CNS pharmacokinetics using a physiologically-based pharmacokinetic modeling approach. Eur. J. Pharm. Sci. 112. https://doi.org/10.1016/j.ejps.2017.11.011.
Zhang, L., Ong, W.Y., Lee, T., 1999. Induction of P-glycoprotein expression in astrocytes following intracerebroventricular kainate injections. Exp. Brain Res. 126, 509–516. https://doi.org/10.1007/s002210050759.